HHS Public Access

Author manuscript

J Vis Exp. Author manuscript; available in PMC 2020 March 26.

Extraction of extracellular vesicles from whole tissue

Stephanie N. Hurwitz, **James M. Olcese**, **David G. Meckes Jr.**

Department of Biomedical Sciences, Florida State University College of Medicine, Tallahassee, FL, USA

Abstract

Circulating and interstitial small membrane-bound extracellular vesicles (EVs) represent promising targets for the development of novel diagnostic or prognostic biomarker assays, and likely serve as important players in the progression of a vast spectrum of diseases. Current research is focused on the characterization of vesicles secreted from multiple cell and tissue types in order to better understand the role of EVs in the pathogenesis of conditions including neurodegeneration, inflammation, and cancer. However, globally consistent and reproducible techniques to isolate and purify vesicles remain in progress. Moreover, methods for extraction of EVs from solid tissue *ex vivo* are scarcely described. Here, we provide a detailed protocol for extracting small EVs of interest from whole fresh or frozen tissues, including brain and tumor specimens, for further characterization. We demonstrate the adaptability of this method for multiple downstream analyses, including electron microscopy and immunophenotypic characterization of vesicles, as well as quantitative mass spectrometry of EV proteins.

SUMMARY:

Here we provide a detailed protocol to isolate small extracellular vesicles (EVs) from whole tissues, including brain and tumor specimens. This method offers a reproducible technique to extract EVs from solid tissue for further downstream analyses.

Keywords

Exosomes; extracellular vesicle; tissue; brain; tumor; mass spectrometry; density gradient; *ex vivo*; oncosomes; biomarkers

INTRODUCTION:

Small extracellular vesicles (EVs) include endosomal-derived exosomes and small membrane-shed microvesicles that are of broad biomedical interest. Small EVs are composed of a heterogeneous population of 50–250 nm membrane-bound vesicles containing biologically active proteins, lipids, and nucleic acids that are collectively believed to play important roles in a multitude of disease processes. Advancing research has

Corresponding Authors: James M. Olcese, David G. Meckes Jr., James.olcese@med.fsu.edu and/or david.meckes@med.fsu.edu.

DISCLOSURES:

The authors have nothing to disclose.

particularly implicated these vesicles in neurodegenerative and prion disorders, infectious processes, autoimmune or inflammatory conditions, and tumor growth and metastasis[1–13]. Rapidly growing biomedical research into the significance of EVs in disease pathogenesis has generated parallel interest in developing reproducible and rigorous methods for the isolation and purification of these vesicles.

A historical and current challenge in EV characterization has been the inability to fully separate small EV subpopulations. This challenge is largely due to our limited understanding of the differing molecular mechanisms governing the biogenesis of distinct vesicles. Overlapping size, density, and biologic cargo between subpopulations further convolutes these distinctions. Part of this challenge has also been the use of widely differing enrichment techniques, providing inconsistency in downstream analysis of isolated vesicles across laboratories, and undermining the global effort to illuminate categorical EV populations.

It is worth noting that the majority of EV characterization has been performed from *in vitro* collection of cell culture supernatant, with more recent *in vivo* studies describing techniques to isolate vesicles from animal or human body fluids, including plasma, urine, and saliva. While EVs are present in large quantities in circulation, it also recognized that these vesicles play important roles in cell-to-cell communication events and are present in the interstitium of cellular tissues. In the context of cancer, interstitial EVs may be particularly important in modulating the tumor microenvironment for cancer cell seeding and metastatic growth[14,15]. Consequently, there is value in the development and optimization of techniques to extract vesicles from solid tissue specimens. These methods will provide a means to directly study organ- or tumor- derived EVs harvested from clinical specimens, including small biopsies and partial or full organ resections.

In this study, and in a previous report published by our laboratory[16], we aim to address several major current concerns in EV enrichment methodology: 1) to describe a reproducible technique to isolate and purify EVs to the highest standards currently accepted in the field; 2) to attempt to isolate small EV subpopulations highly enriched in endosomal-derived exosomes; and 3) to provide a protocol for the extraction of these vesicles from solid tissue specimens for the purpose of further characterization.

Recently, Kowal and colleagues described a relatively small-scale iodixanol density gradient to separate and purify EV subpopulations with greater efficacy than comparable sucrose density gradients[17]. In the cited study, dendritic cell-derived EVs captured in a relatively light density fraction, consistent with a density of 1.1 g/mL, were highly enriched in endosomal proteins believed to be most consistent with a high proportion of exosomes present in this fraction. According to the authors, these “bona fide” exosomal proteins included tumor susceptibility gene 101 (TSG101), syntenin-1, CD81, ADAM10, EHD4, and several annexin proteins[17]. We later adapted this technique to succeed a method of tissue dissociation described by Perez-Gonzalez et al[18] and a subsequent differential centrifugation protocol to isolate whole brain-derived EVs[16]. We also demonstrated the utility of this method in characterizing EV proteomes by combining a sequential protocol for downstream quantitative and comparative mass spectrometry of vesicular protein, previously described

by our laboratory[19]. This work paralleled that from the Hill laboratory, in which EVs were enriched from the frontal cortex of brains[20].

In this study, we elaborate on this technique and extend the application of the protocol recently published from our laboratory to the isolation of EVs from solid lung tumors. To our knowledge, this is the first study to describe a protocol to enrich EVs from *ex vivo* tumor specimens. Given the widespread interest in EVs as novel diagnostic biomarkers and their role in tumorigenesis, this method will likely prove valuable to a growing number of scientific researchers. From a clinical perspective, interstitial EVs could harbor great diagnostic value, particularly in specimens where histologic evaluation is limited. Our hope is that the method outlined here will provide a foundation for a reproducible technique to harvest EVs from fresh or frozen animal or human surgical specimens, paving the way for future work to uncover the significant roles in disease pathogenesis these small vesicles may play.

PROTOCOL:

Whole brains were obtained with approval from the Institutional Animal Use and Care Committee (IACUC) of the Florida State University. A total of twelve mouse brains (3 brains from each age group: 2, 4, 6, and 8 months) from a C57BL/6 J background were used for EV extraction, as previously described[16]. Lung tumor specimens were generously donated by Dr. Mandip Sachdeva under approval of the Florida Agricultural and Mechanical University IACUC. Lung tumors were derived from the human adenocarcinoma cell line H1975 grown in immunodeficient Balb/c nu/nu nude mice. Data from two representative tumor replicates are highlighted in this study.

NOTE: A schematic overview of the vesicle isolation and purification method is provided in Figure 1.

1. Tissue dissociation and differential centrifugation

1.1. Prepare 10 mL of dissociation buffer [10 mg papain; 5.5 mM L-cysteine; 67 μM 2-mercaptoethanol; 1.1 mM EDTA] in Hibernate-E medium per approximately 0.4–1.0 g of tissue. Note that all solutions used for EV enrichment and purification should be diluted in ultrapure filtered water.

1.2. Add whole fresh or frozen tissue to dissociation buffer in a 50 mL conical tube, and incubate in a warm water bath at 37 °C for 20 min. Tissue may be cut into smaller fragments before incubation if needed.

1.3. Following the incubation, add protease and phosphatase inhibitors for a final 1X concentration to the dissociation buffer containing the tissue.

1.4. Pour the solution containing the tissue into a loose-fit Dounce homogenizer, and gently dissociate the tissue using approximately 30 slow strokes per sample. The number of strokes may be adjusted based on tissue consistency.

1.5. Transfer dissociated tissue in buffer to a 50 mL conical tube and centrifuge at 500 × g for 5 min at 4 °C to pellet cells and remaining fibrous or cohesive tissue fragments.

1.6. Transfer the supernatant to a clean 50 mL conical tube and centrifuge at 2,000 × g for 10 min at 4 °C to pellet and discard large cellular debris.

1.7. Transfer the supernatant again to a clean 50 mL conical tube and centrifuge at 10,000 g for 40 min at 4 °C to pellet undesired larger vesicles or small apoptotic bodies.

Note: this pellet can be saved for additional study of larger vesicles if desired.

1.8. Decant supernatant through a 0.45 μm filter into a clean 12 mL ultracentrifugation tube.

Note: densely fibrotic tissue samples may not be easily filtered. These samples can be filtered through a 40 μm cell strainer, then passed through serially smaller needles (18-gauge, 20-gauge, 22-gauge) before filtering through the 0.45 μm filter.

1.9. Ultracentrifuge the sample at 100,000 × g for 2 h at 4 °C to pellet small EVs.

1.10. Decant supernatant and leave the ultracentrifugation tubes inverted for 5–10 min, tapping frequently to remove residual liquid on the sides of tubes. Residual fluid can also be aspirated using an aspirating vacuum pipette.

1.11. Re-suspend EV pellet in 1.5 mL of 0.25 M sucrose buffer [in 10 mM Tris, pH 7.4]. It is important to ensure full re-suspension of the pellet in this step. To do so, cover tubes with parafilm before vortexing EVs into solution. Rock ultracentrifuge tubes for 15–20 min at room temperature before a final vortex mix.

1.12. Briefly centrifuge tubes at a speed no more than 1,000 × g to recover the liquid suspension at the bottom of the tube.

1.13. Proceed to the gradient purification steps below, or if needed, store EV suspension at 4 °C overnight.

2. Density gradient purification

2.1. Add 1.5 mL of 60% iodixanol (stock solution in water) to the 1.5 mL sucrose/Tris buffer containing EVs to create a final solution containing 30% iodixanol. Pipette up and down several times to mix solution thoroughly. Be cautious to avoid losing solution in the pipette tip, as the high iodixanol concentration is quite viscous.

2.2. Transfer the 30% iodixanol buffer solution containing EVs to the bottom of a 5.5 mL ultracentrifugation tube.

2.3. Prepare at least 1.5 mL of 20% and 10% iodixanol solutions per sample in ultrapure water from the 60% iodixanol stock solution.

2.4. Measure 1.3 mL of 20% iodixanol and carefully layer on top of the bottom gradient layer using a syringe and an 18-gauge needle. To avoid mixing the layers at

the density interface, keep the bevel of the needle in contact with the inside of the ultracentrifugation tube just above the meniscus and add the solution dropwise.

2.5. Layer 1.2 mL of 10% iodixanol solution on top of the 20% iodixanol layer using the same technique as above.

2.6. Carefully balance and load the ultracentrifugation tubes into rotor buckets and centrifuge in a swing-bucket rotor at 268,000 × g for 50 min at 4 °C. Set the acceleration and deceleration speeds of the centrifuge to the minimum rates allowed to avoid disruption of the density layers.

2.7. Label ten 1.5 mL microcentrifuge tubes for each sample to correspond to fractions 1 through 10 of the density gradient. Fraction 1 is designated as the topmost fraction that will be first removed, while fraction 10 is the bottom fraction last removed.

2.8. Once the gradient ultracentrifugation has completed, gently remove the tubes from the rotor buckets and place in a stable holder. A visible band of vesicles will often be seen in the fraction of interest. Pipette ten serial fractions of 490 μL from the top of the gradient into the corresponding tubes. There will be a small amount of fluid remaining at the bottom of the tube that likely contains contaminating proteins. This sample can be discarded, or retained as fraction 11 if desired.

2.9. Measure the refractive indices of fractions using a refractometer. This can also be performed with a control gradient run in parallel if sample conservation is necessary. Pipette 20–30 μL of each fraction containing iodixanol onto the refractometer surface, and estimate the density by comparing the refractive indices to known iodixanol densities. Note that fractions can be stored overnight in the iodixanol-containing solution if needed before proceeding to the next ultracentrifugation wash step.

2.10. Transfer each fraction to a clean 12 mL ultracentrifugation tube. Add 5 mL of 1X phosphate-buffered saline [PBS; 137 mM NaCl, 2.7 mM KCl, 10 mM Na2HPO4, 2 mM KH2PO4, pH 7.4] to the tube and mix by pipetting slowly up and down.

Note: PBS added to samples should be particle-free, ensured by filtering sterile PBS through a 0.22 μm filter and storing at room temperature to avoid salt precipitation.

2.11. Add an additional 6 mL of 1X PBS to the top and again mix carefully.

2.12. Ultracentrifuge tubes at 100,000 × g for 2 h at 4°C to re-pellet small vesicles. Decant supernatant and tap tubes dry before lysis of vesicles for protein analysis (Section 3) or re-suspension of EVs for morphologic analysis (Section 5).

3. Lysis and immunoblot confirmation of EV proteins

Note: if preservation of whole vesicles for morphologic characterization or biological activity is desired, researchers can proceed directly to Section 5. In initial experiments, or before mass spectrometry analysis, all fractions recovered should be analyzed by immunoblot to confirm fractions with EV proteins.

3.1. To lyse EVs for protein analysis, add 40 µL of strong lysis buffer [5% SDS, 10 mM EDTA, 120 mM Tris-HCl pH 6.8, 2.5% 2-mercaptoethanol, 8 M urea] with the addition of protease inhibitor to EV pellet in ultracentrifuge tube.

Note: if non-reducing conditions are desired for antibody detection of proteins, substitute ultrapure water for 2-mercaptoethanol in the strong lysis buffer.

3.2. Ensure complete re-suspension of pellet and lysis of EVs in buffer by placing parafilm over the ultracentrifugation tube, vortexing vigorously, then rocking for 20 min at room temperature before a final vortex.

3.3. Briefly centrifuge at 1,000 × g for 30–60 s to recover the entire sample volume. Transfer sample to a new 1.5 mL microcentrifuge tube and store at −20 °C to −80 °C until further processing.

3.4. To prepare purified lysates for immunoblot analysis, add 5X Laemmli sample buffer [10% SDS, 250 mM Tris pH 6.8, 1 mg/mL bromophenol blue, 0.5 M DTT, 50% glycerol, 5% 2-mercaptoethanol] to samples for a final concentration of 1X.

Note: if non-reducing conditions are desired, replace the DTT and 2-mercaptoethanol with ultrapure water.

3.5. If whole tissue homogenate controls are desired, lyse tissue in the urea-containing strong lysis buffer detailed above with protease inhibitor, then centrifuge at 10,000 × g for 10 min to discard remaining extracellular matrix, whole cells, or intact cellular debris. Add 5X Laemmli sample buffer to tissue homogenate for a final concentration of 1X.

3.6. Boil sample buffer containing EV or tissue homogenate samples at 95°C for 5–10 min, then load equal volume (from the equivalent of 0.1–0.3 grams of starting tissue material; 1–2 µg purified EV protein) of fractions 1–10 into a 10% SDS-PAGE gel. Load equal mass of tissue homogenate. Greater volume of samples may be needed for detection by less sensitive antibodies.

3.7. Proceed with gel electrophoresis and western blot analysis as previously detailed[21] to confirm EV proteins in the purified lysates and compare relative EV abundance in fractions.

Note: once EV protein has been reproducibly demonstrated in consistent fractions, the final ultracentrifugation wash described in Step 2.12 may be limited to gradient fractions of interest.

4. EV protein quantification

4.1. Use a detergent- and urea- compatible fluorescence-based assay if sensitive quantification of EV proteins is desired for further analysis (see Table of Materials). Note that some fluorescence-based assays are compatible with the bromophenol blue present in Laemmli sample buffer, facilitating direct lysis of the EV pellet (in Step 2.12) in this buffer if preferred.

4.2. If the aforementioned fluorescence-based protein quantification kit is used, spot 1 μL of sample or standard in at least duplicate on the provided filter paper, and continue protein quantification according to manufacturer's instructions.

5. Characterization of EV morphology

5.1. To examine whole vesicles after the final centrifugation wash in Step 2.12, thoroughly re-suspend EV pellet in particle-free 1X PBS. Store EVs at 4 °C for no longer than one week until processing to avoid freeze-thaw cycles.

Note: It is beneficial to have previously confirmed fractions consistently containing enriched EV protein by immunoblot analysis to limit morphological analyses to fractions of interest.

5.2. Perform nanoparticle tracking analysis on whole EV samples to determine the concentration and size of vesicles in preparations, as previously detailed[22].

5.3. Characterize EV morphology and confirm size measurements by electron microscopy of vesicles, if desired. EM grids can be prepared from vesicle suspensions following Step 5.1[23], or alternatively can be processed as block preparations[24] from pellets following Step 2.12.

6. In-gel purification and trypsin digestion for mass spectrometry analysis

6.1. If characterization of EV proteomes by mass spectrometry is desired, load equal mass (at least 10 μg of protein) of fractions containing EVs into a pre-cast polyacrylamide gel to separate and purify proteins. Manufacturer supplied pre-cast gels are preferred to reduce the levels of potential contaminating proteins (e.g., keratin) being introduced into the samples.

6.2. Run sample at least 0.5 inches into the polyacrylamide gel for protein purification, then fix and stain with Coomassie dye, as previously described in detail[25].

6.3. Cut lanes into 1 mm^3 cubes for trypsin digestion, as previously detailed[19,26].

6.4. Load 5 μL of digested peptide sample into LC-MS/MS instrument for separation on the analytical column and subsequent analysis by mass spectrometry according to parameters specified in detail[16].

REPRESENTATIVE RESULTS:

A schematic overview of the tissue dissociation, differential centrifugation, and gradient purification of vesicles is displayed in Figure 1. The morphologic and immunophenotypic confirmation of gradient-purified EVs is highlighted in Figure 2. A diagram of reproducible densities following ultracentrifugation of the 10–30% iodixanol gradient is shown, with two distinct vesicle populations migrating upward to fraction 2 (light EVs) and fraction 5 (dense EVs), dependent on tissue type. Representative immunoblots of gradient fractions exhibit the efficient separation and purification of small tumor-derived EVs in fraction 5. Of note, lung tumor specimens appeared enriched in dense EVs compared to light EVs (in fraction 2)

previously harvested from whole brain tissue, again highlighted here. As a global tissue analysis of EVs emerge, it will be interesting to determine the distinct densities of EVs produced by unique tissues. Representative nanoparticle tracking analyses and electron microscopy of tissue-derived vesicles in the predominant vesicle-containing fraction demonstrate the enrichment and preservation of whole vesicles consistent with the known size and structure of small EVs. Finally, Figure 3 highlights the utility of this method in facilitating downstream mass spectrometry characterization of gradient-purified vesicle proteins, demonstrating the detection of many proteins previously identified in small EVs. Many of these identified proteins are consistent with those enriched in small endosomal-derived EVs previously proposed by the Théry and Hill labs[17,20].

DISCUSSION:

Much scientific interest has been generated with regards to the roles small EVs play in the tumor microenvironment, as well as in organ development, maturation, and function. Overall, this study provides an optimized workflow for the extraction of intact EVs from whole brain or tumor specimens. While here we simply demonstrate the applicability of this technique to lung tumor-derived EVs, this method could easily be adapted for work on other solid tissues, providing opportunities for further *ex vivo* characterization of small secreted vesicles that are of broad biomedical interest. While beyond the scope of this study, future comparison of EV content to that of originating tissue expression will also be important to establish the utility of isolated vesicles as tissue and disease biomarkers.

In the study previously published by our laboratory, we clearly demonstrate the advantages of the floatation-based density gradient over sedimentation gradients for purification of enriched small vesicles. In essence, a buoyancy-based separation improves purification of vesicles by avoiding contaminant migration through the fractions of interest. This principle appears particularly important when starting from complex samples like whole tissue. Regardless, we stress the importance of the pre-analytical confirmation studies of isolated vesicles described, including examination of EV morphology through complementary techniques such as electron microscopy and nanoparticle tracking analysis, as well as biochemical analyses including immunoblotting. EV proteins in enriched fractions should be confirmed with at least three recognized EV markers, including one tetraspanin protein, as recommended by the *Minimal Information for Studies of EVs* (MISEV) report published in the Journal of Extracellular Vesicles[27]. A negative EV marker should be demonstrated to be absent or highly reduced in EV fractions compared to tissue homogenates. All steps stated above are crucial for quality assurance of small vesicle purification. In addition, early demonstration of laboratory- and user- specific consistency in EV-containing density fractions can save valuable time and cost associated with processing and analyzing all fractions following the density gradient ultracentrifugation step.

It is clear that vesicles from diverse tissues may float to slightly different density fractions, or may separate into predominately light or dense subpopulations. These differences have been previously seen in whole brain-derived EVs compared to EVs harvested from dendritic cells grown in culture[16,17], and are further demonstrated in this study. We show that lung tumor specimens may harbor predominately dense small EVs compared to the lighter EVs

isolated from brain tissue. These differences highlighted by the method proposed in this study may promote valuable inquiries into the differential composition of EVs, including tumor EVs that may be packed with dense DNA strands[28–30]. Because of these differences in EV composition, we strongly underscore the importance of these initial technical experiments. Future application of this technique to the isolation of EVs from diverse tumor specimens will be important to determine if dense EVs are predominately secreted in the interstitium of other tumor types as well.

While the complete purification of small EVs and isolation of distinct vesicle subpopulations remains a current limitation across laboratories, this method provides a basis for further studies to characterize small vesicles from a diversity of tissue or tumor types, and may therefore facilitate a greater understanding of EV diversity. Recent separation of EV particles by asymmetric-flow field-flow fractionation has illuminated the possibility of distinct cargo and functions of small (60–80 nm) versus larger (90–120 nm) exosomes, and further identified a subset of non-membrane bound <50 nm particles denominated as "exomeres"[31,32]. However, cargo packaged in these unique vesicle populations varied across cell lines, highlighting the substantial heterogeneity of secreted vesicles, and supporting the importance of comprehensive *in vitro* or *ex vivo* vesicle analysis. In this study, we most likely enrich for both classes of exosomes identified. A proportion of small microvesicles with similar densities to exosomes may be present in isolates as well. Although we cannot exclude the possibility of exomeres in our isolates, membrane-bound vesicles were certainly most abundant in the gradient fractions enriched in vesicle protein. In addition to small EVs, large oncosomes (> 1,000 nm) have been of recent interest to cancer biologists[33]. While the protocol described in this study filters out vesicles greater than 450 nm, exclusion of this step may facilitate examination of these larger EVs described. Future examination of densities associated with various vesicle subpopulations will be important to distinguish these entities in addition to their described sizes.

Finally, though we appreciate the limitations including cost and time associated with this proposed technique, we also acknowledge the need for rigorous foundational methods to characterize tissue EVs and to serve as an end-product comparison for constantly evolving and more sophisticated methods in the future. These advancing technologies will hopefully illuminate more rapid and clinically-compatible techniques to extract EVs from medical or surgical specimens.

ACKNOWLEDGMENTS:

The authors thank Dr. Richard Nowakowski and the Florida State University Laboratory Animal Resources for providing and caring for the animals used to develop this protocol, respectfully. We thank Xia Liu, Dr. Rakesh Singh, and the Florida State University Translational Science Laboratory for assistance with the mass spectrometry work used for downstream vesicle characterization, as well as the FSU Biological Science Imaging Resource facility for the usage of the transmission electron microscope in this study. Finally, we thank Dr. Mandip Sachdeva (Florida A&M University) for donation of the tumor specimens used in the development of this method. This study was supported by grants from the Florida Department of Health Ed and Ethel Moore Alzheimer's Disease Research Program awarded to D.G.M. and J.M.O (6AZ11) and the National Cancer Institute of the National Institutes of Health under Award Number R01CA204621 awarded to D.G.M.

REFERENCES:

1. Bobrie A, Colombo M, Raposo G & Théry C Exosome secretion: molecular mechanisms and roles in immune responses. Traffic. 12 (12), 1659–1668, doi:10.1111/j.1600-0854.2011.01225.x, (2011). [PubMed: 21645191]
2. Théry C, Zitvogel L & Amigorena S Exosomes: composition, biogenesis and function. Nature Reviews Immunology. 2 (8), 569–579, doi:10.1038/nri855, (2002).
3. Howitt J & Hill AF Exosomes in the Pathology of Neurodegenerative Diseases. Journal of Biological Chemistry. 291 (52), 26589–26597, doi:10.1074/jbc.R116.757955, (2016). [PubMed: 27852825]
4. Sardar Sinha M et al. Alzheimer's disease pathology propagation by exosomes containing toxic amyloid-beta oligomers. Acta Neuropathologica. 136 (1), 41–56, doi:10.1007/s00401-018-1868-1, (2018). [PubMed: 29934873]
5. Meckes DG & Raab-Traub N Microvesicles and viral infection. Journal of Virology. 85 (24), 12844–12854, doi:10.1128/JVI.05853-11, (2011). [PubMed: 21976651]
6. Meckes DG Exosomal communication goes viral. Journal of Virology. 89 (10), 5200–5203, doi:10.1128/JVI.02470-14, (2015). [PubMed: 25740980]
7. Schorey JS, Cheng Y, Singh PP & Smith VL Exosomes and other extracellular vesicles in host-pathogen interactions. EMBO Reports. 16 (1), 24–43, doi:10.15252/embr.201439363, (2015). [PubMed: 25488940]
8. Zhang X et al. Exosomes in cancer: small particle, big player. Journal of Hematology Oncology. 8 83, doi:10.1186/s13045-015-0181-x, (2015). [PubMed: 26156517]
9. Janas AM, Sapoń K, Janas T & Stowell MH Exosomes and other extracellular vesicles in neural cells and neurodegenerative diseases. Biochimica et Biophysica Acta. 1858 (6), 1139–1151, doi:10.1016/j.bbamem.2016.02.011, (2016). [PubMed: 26874206]
10. Chahar HS, Bao X & Casola A Exosomes and Their Role in the Life Cycle and Pathogenesis of RNA Viruses. Viruses. 7 (6), 3204–3225, doi:10.3390/v7062770, (2015). [PubMed: 26102580]
11. Pegtel DM, Peferoen L & Amor S Extracellular vesicles as modulators of cell-to-cell communication in the healthy and diseased brain. Philosophical Transactions of the Royal Society B: Biological Sciences. 369 (1652), doi:10.1098/rstb.2013.0516, (2014).
12. Raposo G et al. B lymphocytes secrete antigen-presenting vesicles. Journal of Experimental Medicine. 183 (3), 1161–1172 (1996). [PubMed: 8642258]
13. Katsiougiannis S Extracellular Vesicles: Evolving Contributors in Autoimmunity. Forum on immunopathological diseases and therapeutics 6 (3–4), 163–170, doi:10.1615/ForumImmunDisTher.2016016491, (2015). [PubMed: 28435748]
14. Costa-Silva B et al. Pancreatic cancer exosomes initiate pre-metastatic niche formation in the liver. Nature Cell Biology. 17 (6), 816–826, doi:10.1038/ncb3169, (2015). [PubMed: 25985394]
15. Hoshino A et al. Tumour exosome integrins determine organotropic metastasis. Nature. 527 (7578), 329–335, doi:10.1038/nature15756, (2015). [PubMed: 26524530]
16. Hurwitz SN et al. An optimized method for enrichment of whole brain-derived extracellular vesicles reveals insight into neurodegenerative processes in a mouse model of Alzheimer's disease. Journal of Neuroscience Methods. 307 210–220, doi:10.1016/j.jneumeth.2018.05.022, (2018). [PubMed: 29894726]
17. Kowal J et al. Proteomic comparison defines novel markers to characterize heterogeneous populations of extracellular vesicle subtypes. Proceedings of the National Academy of Sciences. 113 (8), E968–977, doi:10.1073/pnas.1521230113, (2016).
18. Perez-Gonzalez R, Gauthier SA, Kumar A & Levy E The exosome secretory pathway transports amyloid precursor protein carboxyl-terminal fragments from the cell into the brain extracellular space. Journal of Biological Chemistry. 287 (51), 43108–43115, doi:10.1074/jbc.M112.404467, (2012). [PubMed: 23129776]
19. Hurwitz SN & Meckes DG An Adaptable Polyethylene Glycol-Based Workflow for Proteomic Analysis of Extracellular Vesicles. Methods in Molecular Biology. 1660 303–317, doi:10.1007/978-1-4939-7253-1_25, (2017). [PubMed: 28828667]

20. Vella LJ et al. A rigorous method to enrich for exosomes from brain tissue. Journal of Extracellular Vesicles. 6 (1), 1348885, doi:10.1080/20013078.2017.1348885, (2017). [PubMed: 28804598]
21. Hurwitz SN et al. CD63 Regulates Epstein-Barr Virus LMP1 Exosomal Packaging, Enhancement of Vesicle Production, and Noncanonical NF-κB Signaling. Journal of Virology. 91 (5), doi:10.1128/JVI.02251-16, (2017).
22. Hurwitz SN, Conlon MM, Rider MA, Brownstein NC & Meckes DG Nanoparticle analysis sheds budding insights into genetic drivers of extracellular vesicle biogenesis. Journal of Extracellular Vesicles. 5 31295 (2016). [PubMed: 27421995]
23. Lässer C, Eldh M & Lötvall J Isolation and characterization of RNA-containing exosomes. Journal of Visualized Experiments. (59), e3037, doi:10.3791/3037, (2012). [PubMed: 22257828]
24. Jung MK & Mun JY Sample Preparation and Imaging of Exosomes by Transmission Electron Microscopy. Journal of Visualized Experiments. (131), doi:10.3791/56482, (2018).
25. Meckes DG Affinity purification combined with mass spectrometry to identify herpes simplex virus protein-protein interactions. Methods in Molecular Biology. 1144 209–222, doi:10.1007/978-1-4939-0428-0_14, (2014). [PubMed: 24671686]
26. Rider MA, Hurwitz SN & Meckes DG ExtraPEG: A Polyethylene Glycol-Based Method for Enrichment of Extracellular Vesicles. Scientific Reports 6 23978, doi:10.1038/srep23978, (2016). [PubMed: 27068479]
27. Lötvall J et al. Minimal experimental requirements for definition of extracellular vesicles and their functions: a position statement from the International Society for Extracellular Vesicles. Journal of Extracellular Vesicles. 3 26913 (2014). [PubMed: 25536934]
28. Thakur BK et al. Double-stranded DNA in exosomes: a novel biomarker in cancer detection. Cell Research. 24 (6), 766–769, doi:10.1038/cr.2014.44, (2014). [PubMed: 24710597]
29. Balaj L et al. Tumour microvesicles contain retrotransposon elements and amplified oncogene sequences. Nature Communications. 2 180, doi:10.1038/ncomms1180, (2011).
30. Skog J et al. Glioblastoma microvesicles transport RNA and proteins that promote tumour growth and provide diagnostic biomarkers. Nature Cell Biology. 10 (12), 1470–1476, doi:10.1038/ncb1800, (2008). [PubMed: 19011622]
31. Zhang H et al. Identification of distinct nanoparticles and subsets of extracellular vesicles by asymmetric flow field-flow fractionation. Nature Cell Biology. 20 (3), 332–343, doi:10.1038/s41556-018-0040-4, (2018). [PubMed: 29459780]
32. Zijlstra A & Di Vizio D Size matters in nanoscale communication. Nature Cell Biology. 20 (3), 228–230, doi:10.1038/s41556-018-0049-8, (2018). [PubMed: 29476154]
33. Meehan B, Rak J & Di Vizio D Oncosomes - large and small: what are they, where they came from? Journal of Extracellular Vesicles. 5 33109, doi:10.3402/jev.v5.33109, (2016). [PubMed: 27680302]

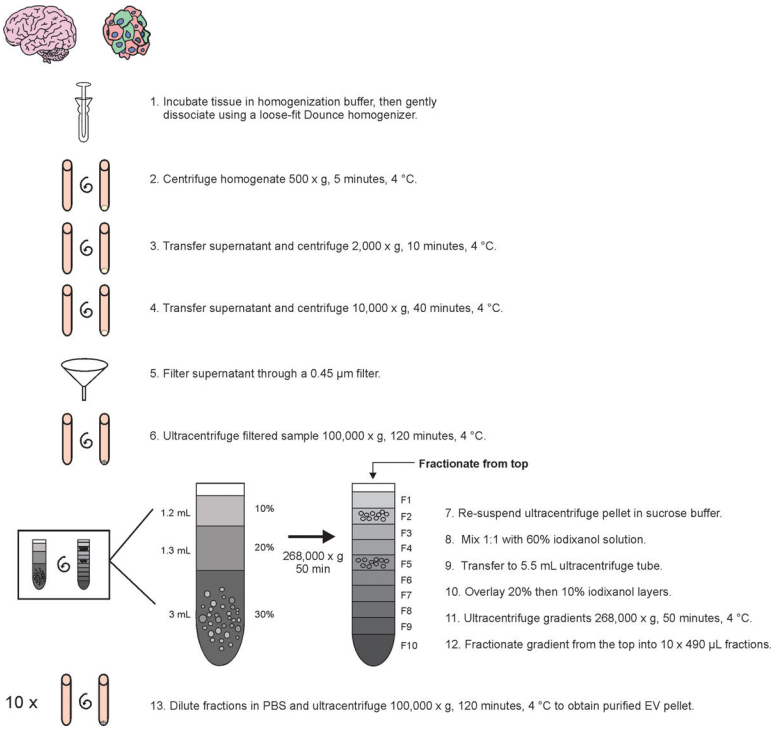

Figure 1. Schematic overview of vesicle isolation and purification from whole tissue.

Following tissue dissociation, pre-clearing differential centrifugation steps, filtration, and ultracentrifugation, crude EV pellets can be resuspended on the bottom of an iodixanol density gradient for floatation separation.

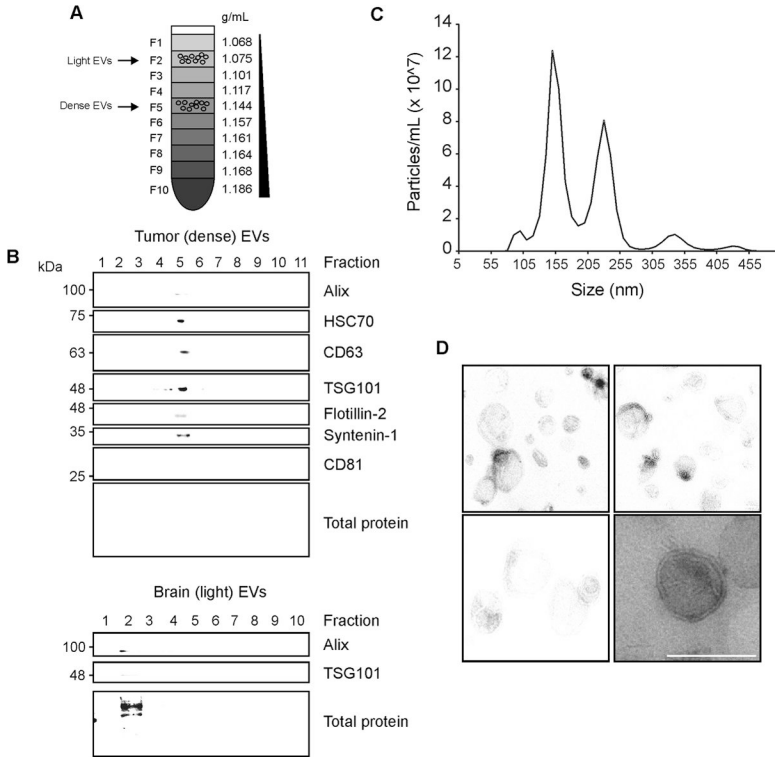

Figure 2. Representative morphologic and immunophenotypic analysis of tissue-derived EVs.

A) Calculated densities of iodixanol gradient following ultracentrifugation, averaged over independent experiments, highlighting fractions containing light and dense EVs. B) Representative immunoblots of tissue-derived vesicles demonstrating the isolation of predominately dense tumor EVs and light brain EVs. Vesicle isolates are depleted of non-EV protein calnexin. *H*, tissue homogenate. C) Nanoparticle tracking analysis (NTA) of representative gradient-purified tissue EVs. The smallest detected particle in this sample was 78 nm, and approximately 92% of vesicles detected were 250 nm or smaller, consistent with a high enrichment of small EVs. D) Representative electron microscopy images of brain tissue-derived EVs. Scale bars = 200 nm.

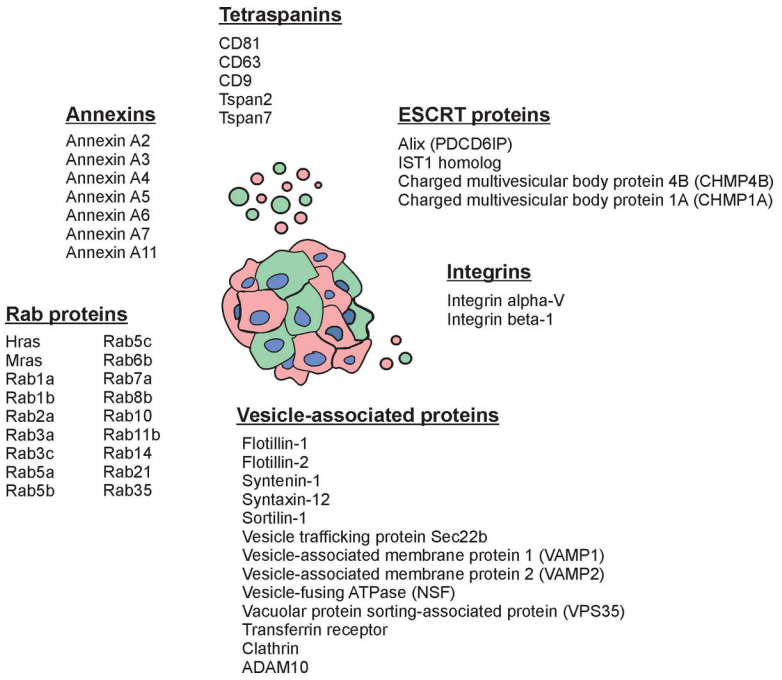

Figure 3. Summary of highlighted vesicle proteins detected by mass spectrometry of a representative tissue-derived EV sample.

Following EV extraction and gradient purification, 10 μg of EV protein in enriched fraction was loaded into a polyacrylamide gel for electrophoresis and in-gel trypsin digestion. In this representative tissue-derived EV sample, a total of 918 proteins were identified by LC-MS/MS analysis. Peptides were identified, analyzed, and found to be enriched in exosomal, lysosomal, and plasma membrane proteins as previously described[16]. Here we demonstrate the presence of small EV or exosomal proteins in our preparations that have been described by the Théry and Hill labs[17,20].

Name of Material/ Equipment	Company	Catalog Number	Comments/Description
0.45 μm filter	VWR	28145–505	
12 mL ultracentrifuge tubes	Beckman Coulter	331372	
5.5 mL ultracentrifuge tubes	Beckman Coulter	344057	
anti-Alix antibody	Santa Cruz	sc-7129	
anti-Calnexin antibody	Santa Cruz	sc-11397	
anti-CD63 antibody	Abcam	ab59479	
anti-CD81 antibody	Santa Cruz	sc-9158	
anti-Flotillin 2 antibody	Santa Cruz	sc-25507	
anti-HSC70 antibody	Santa Cruz	sc-7298	
anti-Syntenin-1 antibody	Santa Cruz	sc-100336	
anti-TSG101 antibody	Santa Cruz	sc-7964	
Dounce homogenizer	DWK Life Sciences	885300–0015	Loose-fit pestle (clearance of 0.889–0.165 mm) used.
EZQ protein quantification kit	ThermoFisher Scientific	R33200	
FA-45-6-30 rotor	Eppendorf	5820715006	
FEI CM120 Electron Microscope	TSS Microscopy		
goat anti-rabbit IgG (Fab fragment)	Genetex	27171	
HALT phosphatase inhibitor (100x solution)	ThermoFisher Scientific	78420	
HALT protease inhibitor (100x solution)	ThermoFisher Scientific	78438	
Hibernate E medium	ThermoFisher Scientific	A1247601	
MLS-50 swinging-bucket rotor	Beckman Coulter	367280	
NanoSight LM10	Malvern		
Optima MAX-XP Benchtop Ultracentrifuge	Beckman Coulter	393315	
Optima XE-100 ultracentrifuge	Beckman Coulter	A94516	
Optiprep	Sigma	D1556	60% iodixanol in sterile water solution
Q Exactive HF Mass Spectrometer	ThermoFisher Scientific		
rabbit anti-goat IgG	Genetex	26741	
rabbit anti-mouse IgG	Genetex	26728	
Refracto 30PX (refractometer)	Mettler Toledo	51324650	

Name of Material/ Equipment	Company	Catalog Number	Comments/Description
S-4-104 rotor	Eppendorf	5820759003	
SW 41 Ti swinging-bucket Rotor	Beckman Coulter	333790	
Tabletop 5804R centrifuge	Eppendorf	22623508	